Journal of Thermal Analysis and Calorimetry
https://doi.org/10.1007/s10973-020-10264-2

Thermal, chemical and antimicrobial characterization of bioactive titania synthesized by sol–gel method

Michelina Catauro[1] · Giovanni Dal Poggetto[2] · Roberta Risoluti[3] · Stefano Vecchio Ciprioti[4]

Received: 10 February 2020 / Accepted: 15 September 2020

Abstract
Chemical stability, anticorrosive properties and photocatalytic activity of titanium dioxide (TiO_2) are among the most important characteristics for industrial and environmental applications. It is well known that titanium biomaterials' properties and response depend significantly on the synthesis method. This work reports the sol–gel synthesis of TiO_2 particles, followed by the studies of their structure, thermal analysis and antimicrobial properties. The main issues were to evaluate the chemical structure of the particles by Fourier transform infrared spectroscopy, the thermal behavior by thermogravimetric analysis and the particle size of the TiO_2 by SEM and BET experiments. In particular, this characterization aims at verifying the possibility to use these materials to prevent infections after implantation. The antibacterial activity of TiO_2 particles was assessed using *Escherichia coli* and *Enterococcus faecalis*. Finally, the bioactivity of TiO_2 particles were estimated by soaking them for 21 days in simulated body fluid with the view to evaluate their biological properties.

Keywords Titanium dioxide · Sol–gel particles · Antibacterial properties · Thermal analysis · Bioactivity

Introduction

Several synthetic routes have been considered in the past to prepare titanium dioxide (TiO_2) nanoparticles, which have been widely considered for many years due to their potential impacts on human life and environment [1]. Titanium dioxide nanomaterials are studied for their several applications, like sunscreens, photovoltaic cells and more other environmental and biomedical applications. The medical applications of TiO_2 are promising, because this material may improve significantly the development of health care [2].

It has been recognized that different synthesis techniques may provide titanium biomaterials with different response and properties [3]. Worth noting among them are ultrasonic spray pyrolysis method [4], semi-batch/batch two stage mixed method [5], microemulsion method [6] and the sol–gel process [7], being the last one the most appropriate one because of the low-temperature condition used [8]. The sol–gel technique is very often selected to produce bulk gels, films, powders and nanoparticles. Furthermore, the structural properties of the so-obtained material are usually affected by different parameters involved in the sol–gel procedure, like the choice of the precursors, the catalysts adopted, the molar ratios of reactants, the solvent composition and the aging and drying conditions [9]. In particular, the versatility, the high degree of purity of the products and the possibility to obtain a fine control of the microstructure of the final product by modulation of the synthesis parameters [10, 11] are the most important advantages of this method.

A growing problem in orthopedics is due to bacterial infection of implantable medical devices, and antibiotic drugs are selected in many patients as the most appropriate therapy after their initial surgery. The antimicrobial resistance and the formation of a biofilm are increasingly prevalent and caused the development of new strategies [12].

✉ Michelina Catauro
michelina.catauro@unicampania.it

✉ Stefano Vecchio Ciprioti
stefano.vecchio@uniroma1.it

[1] Department of Industrial and Information Engineering, University of Campania "Luigi Vanvitelli", Via Roma 29, 81031 Aversa, Italy

[2] Ecoricerche srl, Via Principi Normanni 36, 81043 Capua, Italy

[3] Department of Chemistry, Sapienza University of Rome, P.le A. Moro 5, 00185 Rome, Italy

[4] Department S.B.A.I., Sapienza University of Rome, Via del Castro Laurenziano 7, 00161 Rome, Italy

Published online: 09 October 2020

Photocatalysis is one of the promising methods of disinfection, and several semiconductors have been used as photocatalysts, and among them in particular titanium dioxide, as reported by Guillard et al. [13] and Wu et al. [14]. In fact, the semiconductor properties as well as the excellent photocatalytic activity of TiO_2 are well known and often used in elimination of environmental pollutants [15], antibacterial dopes and self-clean buildings [16]. In addition, this material is a valuable candidate for applications in medical devices and sanitary ware surfaces because of its incomparable antibacterial properties [17].

It is well known that TiO_2 irradiated by UV light produces hydrogen peroxide, hydroxyl radical and superoxide anions (namely reactive oxygen species denoted as ROS) that can be responsible of cell death caused by the decomposition of the cell wall first layer, followed by the decomposition of the cell membrane [18, 19]. Furthermore, the lethal effects exerted by the TiO_2 photocatalytic reaction have also been set up in other kind of cells like as fungi, yeasts, viruses or cancer cells [18].

This investigation aims at preparing (via sol–gel) and characterizing TiO_2 particles in order to evaluate their use to prevent infections after implantation.

Fourier transform infrared (FTIR) spectroscopy and thermogravimetry (TG) were used to evaluate the chemical structure and to interpret the thermal behavior of the particles, while the morphology and their particles have been investigated by scanning electron microscopy (SEM) and Brunauer–Emmet–Teller (BET) analyses. Some years ago the thermal behavior of titania nanoparticles prepared by precipitation from aqueous solutions was investigated [20]. In this previous study, the authors focused their attention on characterizing the materials obtained [using TG–DTA, emanation thermal analysis (ETA), MS detection, FTIR and X-ray diffraction (XRD)] to test their suitability as photocatalysts, neglecting the evaluation of any possible antibacterial property or bioactivity, which are among the main aims of the present investigation. So, the biological properties of the TiO_2 particles with particular reference to their bioactivity were evaluated by soaking them for 21 days in simulated body fluid (SBF). Moreover, the antibacterial activity of TiO_2 particles was assessed using *Escherichia coli* and *Enterococcus faecalis*.

Experimental

Materials

Titanium(IV) butoxide (TBT, Sigma-Aldrich), pure ethanol (99.8% Sigma-Aldrich) were used as received as well as ammonia solution (25% Sigma-Aldrich) and distilled water.

Sol–gel synthesis

In order to prepare TiO_2 particles by the sol–gel method, titanium(IV) butoxide (TBT), precursor of the titanium matrix, was preliminarily added to a solution obtained by mixing pure ethanol and distilled water. The solution containing TBT and ethanol was left under stirring for 15 min, and then, ammonia solution (NH_3H_2O) was added drop by drop. The final molar ratio in the solution was TBT :EtOH:H_2O:NH_3 = 1:20.2:1.5:1. Once ammonia solution ($NH_3 \cdot H_2O$) was added, precipitation was clearly visible, and the product formed was left in an oven at 60 °C for 72 h.

Fourier transform infrared (FTIR) spectroscopy

The chemical structure of TiO_2 particles was evaluated by FTIR analysis using a Prestige 21 (Shimadzu, Japan) system in the 400–4000 cm^{-1} range, with a resolution of 4 cm^{-1}. A DTGS KBr (deuterated triglycine sulfate with potassium bromide windows) detector and 2 mg of sample were used (in the form of pelleted disks diluted with KBr according to a 1:100 sample-to-KBr mass ratio). FTIR spectra were analyzed by Prestige software.

Thermal analysis

TG experiments were carried out using a PerkinElmer TGA7 Thermobalance (Massachusetts, USA) equipped with platinum crucibles. Samples of size of about 3–5 mg were heated up to 1173 K at 10 K min^{-1} (as the best resolution rate) under a pure nitrogen atmosphere at 100 mL min^{-1}. Temperature calibration was carried out by considering the Curie point transition of very pure standard metals or alloys (endpoint temperatures of Ni and alumel at 436 and 627 K, in this study), according to the equipment recommendations. TG data were checked and acquired by Pyris software (Thermo Fisher Scientific Inc., Waltham, MA, USA), and ASCII files were processed by V-JDSU Unscrambler Lite (Camo software AS, Oslo, Norway). Optimal evaluation of initial and final temperatures of each step was obtained by calculating the first order derivative of the TG curve (DTG) as a function of temperature.

Scanning electron microscopy (SEM) and Brunauer–Emmet–Teller (BET) analysis

SEM analysis was performed using an AURIGA Zeiss High Resolution Field Emission instrument (HR-FESEM, JEOL JSM-7000F, Japan). An energy-dispersive X-ray

(EDX) unit was used to investigate the morphology of the titania material prepared.

Before performing the SEM analysis, ethanol suspensions of the particles were prepared and then centrifuged for few minutes to obtain a homogeneous suspension. The particle suspension was transferred on the stub of the SEM using clean glass capillaries. The drying of the sample's suspension on the stub of the SEM occurred very quickly because of the high evaporation rate of ethanol that avoids the agglomeration of particles. Then, micrographs were taken at a number of random locations on the grid.

Porosity and specific surface area of TiO_2 particles were evaluated by BET (Fisons Instruments) analyses at liquid nitrogen temperature. Gaseous nitrogen was used to evaluate the specific surface of powders.

Bioactivity test

A Kokubo test was carried out to evaluate the bioactivity of the TiO_2 particles [21]. The particles were soaked in a simulated body fluid (SBF) for 21 days using ion concentrations approximately equal to those found in human blood plasma. In order to keep the SBF solution temperature quite constant at 37 °C, the samples were transferred in polystyrene bottles and fully immersed in a water bath. Furthermore, in order to avoid depletion of the ionic species caused by the formation of biominerals the SBF solution, in which the particles were soaked, was exchanged every 2 days. After each soaking period, the samples were removed from the SBF, air-dried in a desiccator. Finally, after 24 h they were subjected to FTIR, EDX and XRD analyses in order to evaluate how they are able to form an apatite layer on their surfaces.

Antibacterial properties

The antibacterial properties of the TiO_2 particles were evaluated using Escherichia coli, Gram-negative (ATCC 25922), and *Enterococcus faecalis*, Gram-positive (ATCC 29212). *E. coli* was inoculated in TBX Medium (Tryptone Bile X-Gluc) (Liofilchem, Italy) with the particles for 24 h at 44 °C, whereas *E. faecalis* was inoculated in Slanetz Bartley Agar Base (Liofilchem, Italy), with particles for 48 h at 36 °C. 10×10^5 CFU mL^{-1} bacterial cell suspensions were obtained by diluting the bacterial culture in distilled water. The antibacterial activities were evaluated by observing the different bacterial growths and by measuring the diameter of the inhibition halos (ID) [22]. The values so determined in three replicas are presented as mean standard deviations (SDs) of measurements.

Results and discussion

FTIR analysis

Figure 1 shows the comparison of the FTIR spectrum of TiO_2 particles (pretreated at 60 °C) (namely curve b) and those of ethanol and TBT precursor (curves a and c, respectively). The bands at about 1400 cm^{-1} can be attributed to the bending of $–CH_2$ and $–CH_3$ of the TBT precursor. Furthermore, the bands at 2956 and 2868 cm^{-1} are ascribed to the asymmetric and symmetric stretching modes of the methyl groups [23, 24]. By comparing the spectra of TiO_2 and ethanol, the typical bands related to the C–O group of ethanol at 1126, 1097 and 1037 cm^{-1} are detected [25], while the broad intense band at 3307 cm^{-1} can be due to the stretching of the OH group. According to the results of previous studies [7, 24], the signals in the region spectrum between 1000 and 400 cm^{-1} can be attributed to the bending vibrations of Ti–OH, Ti–O and O–Ti–O bonds.

The results derived by the analysis of the FTIR spectra suggest that the thermal treatment at 60 °C is not able to completely remove the water adsorbed on the materials during the synthesis process. Finally, a confirmation of water weakly bound in the material is obtained by the presence of the band at 1635 cm^{-1} [23].

Thermal analysis

The TG and DTG curves of TiO_2 recorded under inert gas atmosphere (black and gray lines, respectively) are reported in Fig. 2 from ambient temperature to 1123 K. Four steps of mass loss were recorded in the temperature range explored

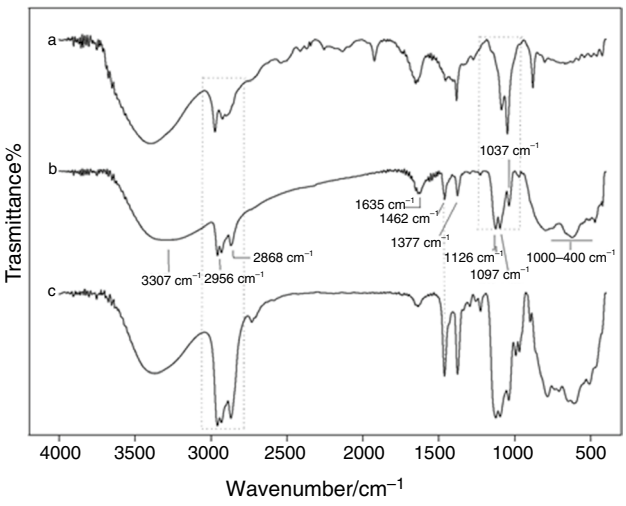

Fig. 1 Representative FTIR spectra a pure ethanol; b TiO_2 particles and c pure TBT

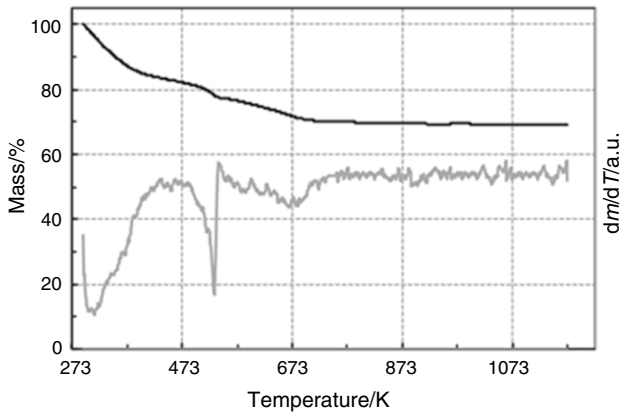

Fig. 2 TG/DTG curves of TiO_2 particles (black and gray lines, respectively)

(corresponding to four downwards peaks of the DTG curve) with a total residue of 31.1%. The first step takes place up to 440 K and can be attributed primarily to the loss of 17.0% of water, without discrimination between physically and chemically bound water, thus confirming the finding of a previous study [20]. In the mentioned study, where TiO_2 was obtained by precipitation from aqueous solutions, a total residue of 31.7% was found, which is in very good agreement with our results. The release of some alcohol (residue of the synthesis and not completely removed) in the first step cannot be excluded, as already found in the case of similar or hybrid materials prepared by the sol–gel method [26, 27].

The second step occurs between 440 and 550 K with a mass loss of 6.7% may be ascribed to the thermal decomposition of ammonium salt (residue of the synthesis that remained in the sol and then in the sample), similarly to what has been found in [20]. The third step that occurs in the range 570–750 K is given by dehydroxylation, which represents the thermal release of water obtained by condensation of hydroxyl groups, as detected in the same temperature range for several glass and hybrid materials [28]. It is worth noting that no mass loss was observed at temperature higher than 800 K.

SEM and BET analysis

The SEM micrographs of the TiO_2 particles are shown in Fig. 3, which show a non-uniform distribution of the particle size (Fig. 3a). Nevertheless, the SEM images also show average particle size of about 700 nm, while the presence of both water molecules and hydroxyl group may explain the fact that no aggregate particles are clearly visible [26–30]. Energy-dispersive X-ray microanalysis (EDX) showed the characteristic peaks of Ti, O and C elements that make up the particles (Fig. 3b). The presence of the peak of carbon is explained by the presence of residual solvent, not completely released by the thermal treatment at 60 °C, as also demonstrated by FTIR analysis.

It is known that the specific surface area (BET) decreases with increasing the particle size of the samples and the degree of agglomeration [26]. In this study, BET testing results indicate that the BET specific surface area of the TiO_2 particles dried at 60 °C for 72 h is about 7.9 $m^2\ g^{-1}$. Comparing these results with those reported by Viana et al. [31] and Wetchakun et al. [32], it can be stressed that the

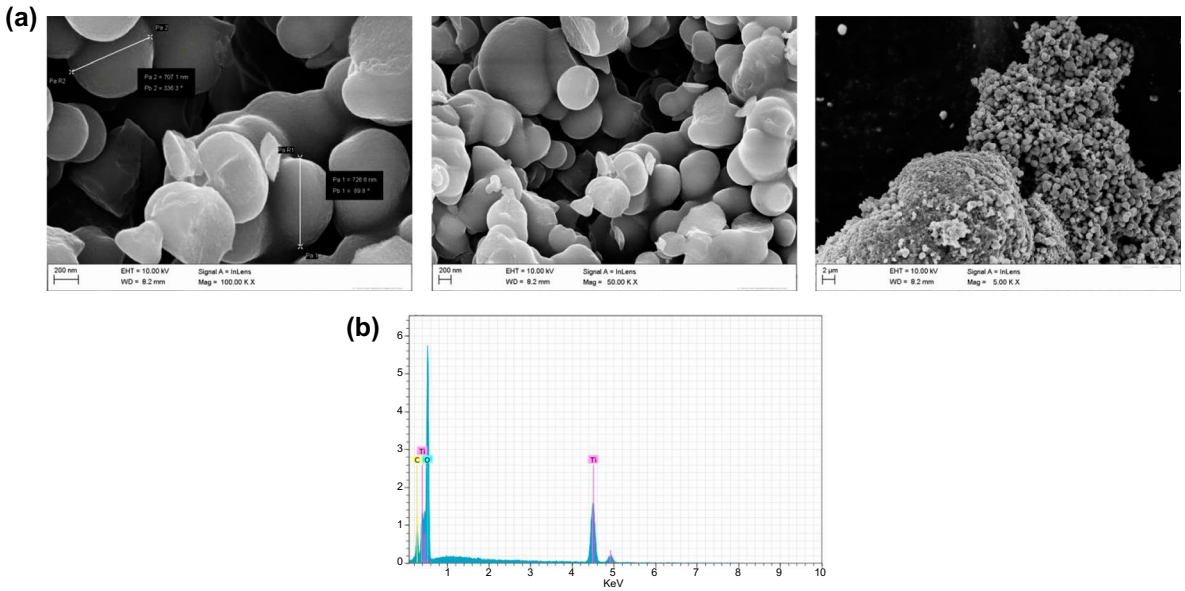

Fig. 3 **a** SEM micrographs of TiO_2 particles, **b** EDX analysis of TiO_2 particles

thermal treatment adopted in this study (i.e., 60 °C for 72 h) negatively affected the size of the particles due to aggregation. In fact, it is reported [33, 34] that the specific surface area and porosity systematically decrease with increasing the temperature of the thermal treatment, thus demonstrating the occurrence of sample densification, followed by a consequent increase in the average particle size. In conclusion, it is possible to obtain smaller particle size avoiding their aggregation using a drying process occurring at low temperature.

Bioactivity test

As stated above, the bioactivity of the particles was evaluated via the Kokubo's test [21] after treatment for 21 days in SBF. According to the studies of Kokubo and his colleagues [21, 35, 36], good performances of a biomaterial require the formation of apatite on its surface after implantation in the human body. A preliminary analysis of this formation was carried out by using FTIR spectroscopy. In particular, the TiO_2 spectra recorded before and after being soaked in the solution are reported in Fig. 4 (plots a and b, respectively). After 21 days in SBF, it is possible to observe the changes of some bands. The stretching of –OH groups of hydroxyapatite and the vibrations of the PO_4^{3-} groups [37], caused by the interaction among the hydroxyapatite precipitate and the matrix [36], are responsible of the change in the shape and the broadening of the bands at about 500 cm^{-1} [33, 38, 39]. The formation of hydroxyapatite can be revealed by the characteristics bands of PO_4^{2-} groups (1000–1100 cm^{-1} asymmetric stretching vibration and 580 cm^{-1} asymmetric bending vibration) and CO_3^{2-} (1380 cm^{-1} stretching vibration) [40].

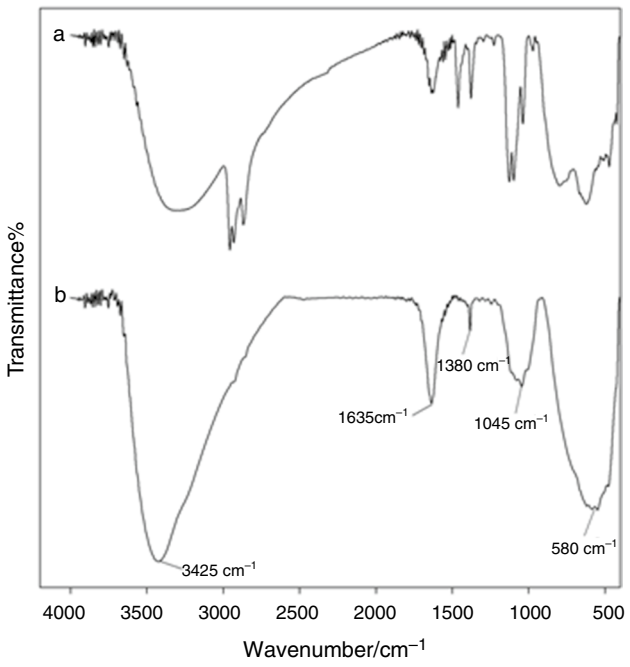

Fig. 4 Representative FTIR spectra a TiO_2 particles not soaked in SBF and b TiO_2 particles after 21 days in SBF

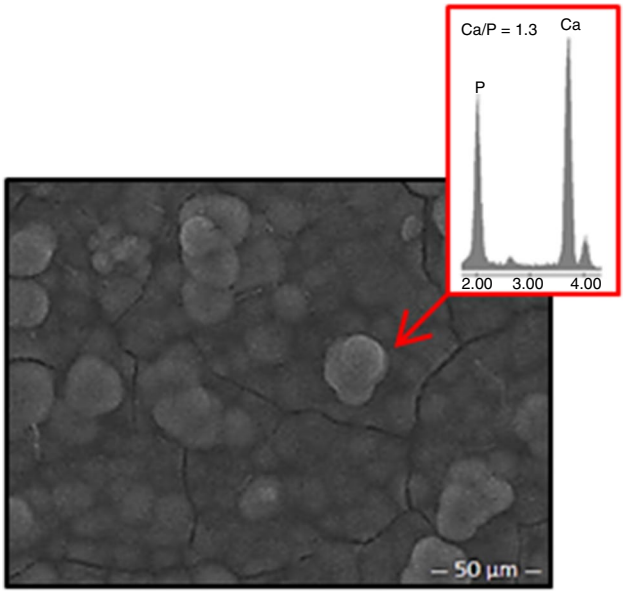

Fig. 5 SEM micrographs of TiO_2 and EDX analysis soaked in SBF solution for 21 days

Nucleation of hydroxyapatite on the surface of the particles is stimulated by the presence of Ti–OH groups [41]. In particular, these groups attract the Ca^{2+} ions present in the fluid, thus provoking an increase in the surface positive charge. Subsequently, an interaction with the negative charge of the phosphate ions is allowed. Finally, amorphous phosphate is formed and spontaneously suddenly converted into hydroxyapatite [$Ca_{10}(PO_4)_6(OH)_2$] [42, 43].

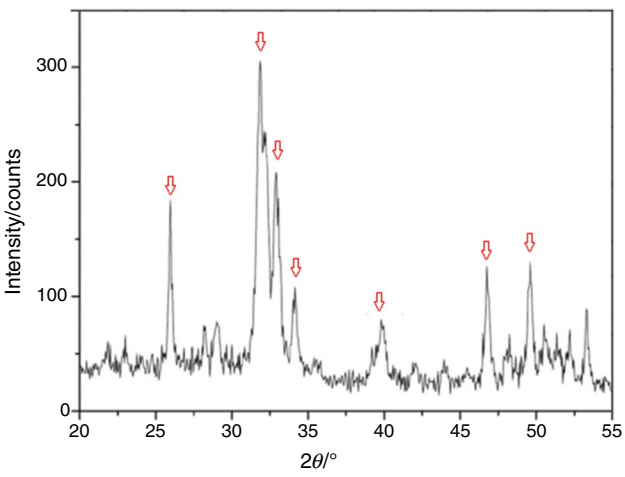

Fig. 6 XRD spectra of TiO_2 particles soaked in SBF solution for 21 days

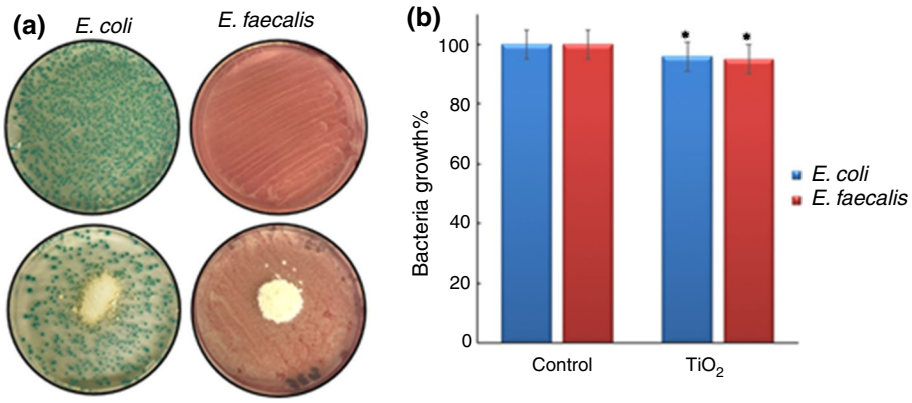

Fig. 7 **a** Image of *E. coli* and *E. faecalis* unexposed to materials and incubated with TiO_2 particles. **b** Bacteria growth (%) of *E. coli and E. faecalis* incubated with and without TiO_2 particles. Values are the mean standard deviation of measurements carried out on samples analyzed three times. The means and standard deviations are shown. $^*p < 0.05$ versus the bacteria treated with particles

FTIR data about the formation of the hydroxyapatite layer on the surfaces of titania particles were confirmed by SEM/EDX analysis (Fig. 5). In EDX microanalysis of TiO_2 after exposure to SBF, mean element peaks are found related to hydroxyapatite formation (Ca and P) with an atomic ratio Ca/P equal to 1.3. Furthermore, the formation of crystalline hydroxyapatite was confirmed by the intense peaks in the XRD spectrum (Fig. 6). In addition, the XRD results suggested that the hydroxyapatite layer on the material's surface was very thick.

Antibacterial properties

Incubation of titania particles has been carried out with Gram-positive and Gram-negative bacterial strains to evaluate their growth. Figure 7a shows the images of *E. coli* and *E. faecalis,* while Fig. 7b shows the progress of bacterial growth. Comparing the results of different bacteria, the inhibition halo (ID) was not observed.

The viability of both bacteria exposed to TiO_2 particles was very similar to that of bacteria unexposed to any materials, used as control. In fact, the results suggest that the particles had no antibacterial property and supported the proliferation of bacteria, regardless of the bacterial strain [44–47]. Therefore, the TiO_2 particles prepared and characterized in the present study may be considered as non-toxic material, suitable for different applications in the biomedical field.

Conclusions

In the present investigation, TiO_2 particles were synthesized by the sol–gel method. The physicochemical and morphological characterization, carried out using FTIR, SEM and BET analyses, revealed that even though the particle size is non-uniform, an average value is found corresponding to about 700 nm. Aggregation of particles is not clearly visible, because of the presence of both water molecules and hydroxyl group, confirmed also by FTIR analysis. Furthermore, both the FTIR spectra and TG experiments suggest that the thermal treatment at 60 °C does not completely remove the water and residue solvents. As a confirmation, the EDX analysis showed both the peaks of Ti and O, as well as those of Carbon. TG experiments revealed that in spite of the thermal pretreatment at 60 °C, a significant mass of water physically or weakly bound to the material was released at low temperature. The occurrence of processes accompanied by mass losses can be excluded at temperature higher than 800 K.

As far as the biological characterization is concerned, the Kokubo test confirmed that the formation of hydroxyapatite layers occurs after 21 days in SBF, thus suggesting that the TiO_2 particles synthesized in this study are bioactive.

Finally, during the incubation of particles with two bacterial strains, namely Gram-positive and Gram-negative, the inhibition halo (ID) was not observed. So, in conclusion it can be stressed that the TiO_2 particles prepared in the present study support the proliferation of bacteria, regardless of the bacterial strain. Therefore, they may be used as non-toxic materials for different biomedical applications.

Funding The work was financially supported by V:ALERE 2019 Grant support from University of Campania "Luigi Vanvitelli" of CHIMERA.

Compliance with ethical standards

Conflict of interest The authors declare that they have no conflict of interest.

References

1. Jin C, Tang Y, Yang F, Lin Li X, Xu S, Yan Fan X, Ying Huang Y, Ji Yang Y. Cellular toxicity of TiO_2 nanoparticles in anatase and rutile crystal phase. Biol Trace Elem Res. 2011;141(1–3):3–15.
2. Ramos AP, Cruz MAE, Tovani CB, Ciancaglini P. Biomedical applications of nanotechnology. Biophys Rev. 2017;9(2):79–89.
3. Kulkarni M, Mazare A, Gongadze E, Perutkova Š, Kralj-Iglič V, Milošev I, Schmuki P, Iglič A, Mozetič M. Titanium

nanostructures for biomedical applications. Nanotechnology. 2015;26(6):062002.
4. Taziwa R, Meyer E. Fabrication of TiO_2 nanoparticles and thin films by ultrasonic spray pyrolysis: design and optimization. In Pyrolysis. Rijeka: InTech; 2017.
5. Do Kim K, Kim HT. Synthesis of TiO_2 nanoparticles by hydrolysis of TEOT and decrease of particle size using a two-stage mixed method. Powder Technol. 2001;119(2–3):164–72.
6. Kim EJ, Hahn S-H. Microstructure and photoactivity of titania nanoparticles prepared in nonionic W/O microemulsions. Mater Sci Eng A. 2001;303(1–2):24–9.
7. Vargas MA, Rodríguez-Páez JE. Amorphous TiO_2 nanoparticles: synthesis and antibacterial capacity. J Non-Cryst Solids. 2017;459:192–205.
8. Catauro M, Laudisio G, Costantini A, Fresa R, Branda F. Low temperature synthesis, structure and bioactivity of 2CaO 3SiO2 glass. J Sol-Gel Sci Technol. 1997;10(2):231–7.
9. Milea C, Bogatu C, Duta A. The influence of parameters in silica sol–gel process. Bull Transilv Univ Brasov. 2011;4:53.
10. Su C, Hong B-Y, Tseng C-M. Sol–gel preparation and photocatalysis of titanium dioxide. Catal Today. 2004;96(3):119–26.
11. Macwan D, Dave PN, Chaturvedi S. A review on nano-TiO_2 sol–gel type syntheses and its applications. J Mater Sci. 2011;46(11):3669–86.
12. Ercan B, Taylor E, Alpaslan E, Webster TJ. Diameter of titanium nanotubes influences anti-bacterial efficacy. Nanotechnology. 2011;22(29):295102.
13. Guillard C, Bui T-H, Felix C, Moules V, Lina B, Lejeune P. Microbiological disinfection of water and air by photocatalysis. C R Chim. 2008;11(1–2):107–13.
14. Wu MJ, Bak T, O'Doherty PJ, Moffitt MC, Nowotny J, Bailey TD, Kersaitis C. Photocatalysis of titanium dioxide for water disinfection: challenges and future perspectives. Int J Photochem. 2014;2014:973484.
15. Shahid M, McDonagh A, Kim JH, Shon HK. Magnetised titanium dioxide (TiO_2) for water purification: preparation, characterisation and application. Desalin Water Treat. 2015;54(4–5):979–1002.
16. Xu X, Wang J, Tian J, Wang X, Dai J, Liu X. Hydrothermal and post-heat treatments of TiO_2/ZnO composite powder and its photodegradation behavior on methyl orange. Ceram Int. 2011;37(7):2201–6.
17. Wanag A, Rokicka P, Kusiak-Nejman E, Kapica-Kozar J, Wrobel RJ, Markowska-Szczupak A, Morawski AW. Antibacterial properties of TiO_2 modified with reduced graphene oxide. Ecotoxicol Environ Saf. 2018;147:788–93.
18. Athanasoulia I-G, Mikropoulou M, Karapati S, Tarantili P, Trapalis C. Study of thermomechanical and antibacterial properties of TiO_2/Poly (lactic acid) nanocomposites. Mater Today Proc. 2018;5(14):27553–62.
19. Moriyama A, Yamada I, Takahashi J, Iwahashi H. Oxidative stress caused by TiO_2 nanoparticles under UV irradiation is due to UV irradiation not through nanoparticles. Chem Biol Interact. 2018;294:144–50.
20. Pulisova P, Bohacek J, Subrt J, Szatmary L, Bezdicka P, Vecernikova E, Balek V. Thermal behaviour of titanium dioxide nanoparticles prepared by precipitation from aqueous solutions. J Therm Anal Calorim. 2010;101:607–13.
21. Kokubo T, Takadama H. How useful is SBF in predicting in vivo bone bioactivity? Biomaterials. 2006;27(15):2907–15.
22. Catauro M, Tranquillo E, Barrino F, Blanco I, Dal Poggetto F, Naviglio D. Drug release of hybrid materials containing Fe(II) Citrate synthesized by sol–gel technique. Materials (Basel). 2018;11(11):2270.
23. Li Z, Zhu Y, Wang J, Guo Q, Li J. Size-controlled synthesis of dispersed equiaxed amorphous TiO_2 nanoparticles. Ceram Int. 2015;41(7):9057–62.
24. Wang Y-d, Ma C-l, Sun X-d, Li H-d. Synthesis and characterization of amorphous TiO_2 with wormhole-like framework mesostructure. J Non-Cryst Solids. 2003;319(1):109–16.
25. Zeitler VA, Brown CA. The infrared spectra of some Ti–O–Si, Ti–O–Ti and Si–O–Si compounds. J Phys Chem. 1957;61(9):1174–7.
26. Viana MM, Soares VF, Mohallem NDS. Synthesis and characterization of TiO_2 nanoparticles. Ceram Int. 2010;36(7):2047–53.
27. Bruno ME, Tasat DR, Ramos E, Paparella ML, Evelson P, Rebagliati RJ, Cabrini RL, Guglielmotti MB, Olmedo DG. Impact through time of different sized titanium dioxide particles on biochemical and histopathological parameters. J Biomed Mater Res Part A. 2014;102(5):1439–48.
28. Rao KS, El-Hami K, Kodaki T, Matsushige K, Makino K. A novel method for synthesis of silica nanoparticles. J Colloid Interface Sci. 2005;209(1):125–31.
29. Lopez T, Jardón G, Gomez E, Gracia A, Hamdan A, LuisCuevas J, Quintana P, Novaro O. Ag/TiO_2–SiO_2 sol gel nanoparticles to use in hospital-acquired infections (HAI). J Mater Sci Eng. 2015;4(6):196.
30. Li J, Zhen D, Sui G, Zhang C, Deng Q, Jia L. Nanocomposite of Cu–TiO_2–SiO_2 with high photoactive performance for degradation of rhodamine B dye in aqueous wastewater. J Nanosci Nanotechnol. 2012;12(8):6265–70.
31. Wetchakun N, Incessungvorn B, Wetchakun K, Phanichphant S. Influence of calcination temperature on anatase to rutile phase transformation in TiO_2 nanoparticles synthesized by the modified sol–gel method. Mater Lett. 2012;82:195–8.
32. Gaber A, Abdel- Rahim MA, Abdel-Latief AY, Abdel-Salam MN. Influence of calcination temperature on the structure and porosity of nanocrystalline SnO_2 synthesized by a conventional precipitation method. Int J Electrochem Sci. 2014;9(1):81–95.
33. Catauro M, Tranquillo E, Risoluti R, Vecchio Ciprioti S. Sol–gel synthesis, spectroscopic and thermal behavior study of SiO_2/PEG composites containing different amount of chlorogenic acid. Polymers. 2018;10:682.
34. Catauro M, Tranquillo E, Dal Poggetto G, Pasquali M, Dell'Era A, Vecchio Ciprioti S. Influence of the heat treatment on the particles size and on the crystalline phase of TiO2 synthesized by the sol–gel method. Materials. 2018;11(12):2364.
35. Kokubo T, Ito S, Huang ZT, Sakka S, Kitsugi T, Yamamuro T. Ca, P-rich layer formed on high-strength bioactive glass-ceramic A-W. J Biomed Mater Res. 1990;24(3):331–43.
36. Kokubo T, Kushitani H, Sakka S, Kitsugi T, Yamamuro T. Solutions able to reproduce in vivo surface-structure changes in bioactive glass-ceramic A-W. J Biomed Mater Res. 1990;24(6):721–34.
37. Catauro M, Tranquillo E, Salzillo A, Capasso L, Illiano M, Sapio L, Naviglio S. Silica/polyethylene glycol hybrid materials prepared by a sol–gel method and containing chlorogenic acid. Molecules. 2018;23(10):2447.
38. Catauro M, Barrino F, Dal Poggetto G, Pacifico F, Piccolella S, Pacifico S. Chlorogenic acid/PEG-based organic–inorganic hybrids: a versatile sol–gel synthesis route for new bioactive materials. Mater Sci Eng C. 2019;100:837–44.
39. Berzina-Cimdina L, Borodajenko N. Research of calcium phosphates using Fourier transform infrared spectroscopy. Infrared Spectrosc Mater Sci Eng Technol. 2012;12(7):251–63.
40. El-Bassyouni GT, Eldera SS, Kenawy SH, Hamzawy EMA. Hydroxyapatite nanoparticles derived from mussel shells for in vitro cytotoxicity test and cell viability. Heliyon. 2020;6(6):e0408.
41. Catauro M, Bollino F, Papale F, Lamanna G. Investigation of the sample preparation and curing treatment effects on mechanical properties and bioactivity of silica rich metakaolin geopolymer. Mater Sci Eng C. 2014;36(1):20–4.

42. Ohtsuki C, Kokubo T, Yamamuro T. Mechanism of apatite formation on $CaOSiO_2P_2O_5$ glasses in a simulated body fluid. J Non-Cryst Solids. 1992;143(1):84–92.
43. Catauro M, Renella RA, Papale F, Ciprioti SV. Investigation of bioactivity and thermal behavior of sol–gel silica glass containing a high PEG percentage. Mater Sci Eng C. 2016;61(1):51–5.
44. Tranquillo E, Barrino F, Dal Poggetto G, Blanco I. Sol–gel synthesis of silica-based materials with different percentages of PEG or PCL and high chlorogenic acid content. Materials. 2019;12(1):155.
45. Catauro M, Barrino F, Dal Poggetto G, Crescente G, Piccolella S, Pacifico S. Chlorogenic acid entrapped in hybrid materials with high PEG content: a strategy to obtain antioxidant functionalized biomaterials? Materials. 2019;12(1):148.
46. Nguyena K, Garcia A, Sanic M-A, Diaza D, Dubeyd V, Claytona D, Dal Poggetto G, Corneliuse F, Paynea RJ, Separovic F, Khandeliad H, Clarke RJ. Interaction of N-terminal peptide analogues of the Na+, K+-ATPase with membranes. BBA-Biomembr. 2018;1860(6):1282–91.
47. Catauro M, Tranquillo E, Barrino F, Dal Poggetto G, Blanco I, Cicala G, Ognibene G, Recca G. Mechanical and thermal properties of fly ash-filled geopolymers. J Therm Anal Calorim. 2019;138(5):3267–76.